High-Power Low-Noise Nd:YAP/LBO Laser with Dual Wavelength Outputs

Yajun Wang, Yaohui Zheng, Changde Xie, and Kunchi Peng

***Abstract*— A high-power single-frequency Nd:YAP/LBO laser with stable dual wavelength outputs is designed and built. The laser resonator satisfying optimal coupling condition for second-harmonic generation is in a configuration of a figure "8" shaped ring cavity consisting of two convex mirrors and two concave mirrors. An additional wedge YVO_4 crystal is inserted in the resonator to act as a polarizer, so that the stability of the laser operation is improved. The maximum output powers of 4.5 W at 540 nm and 1.5 W at 1080 nm are simultaneously achieved. The measured power stabilities of the fundamental wave and the second-harmonic wave are ±0.32% and ±0.6% for 3 h, respectively.**

***Index Terms*— Intracavity second-harmonic generation, laser stability, optical resonators, solid-state ring lasers.**

I. Introduction

ALL-SOLID-STATE single-frequency lasers have attracted a great deal of attentions for their applications in high-resolution laser spectroscopy, nonlinear optics and quantum optics etc. In quantum optics experiments, single-frequency lasers can be used as the pump sources of optical parametric oscillators (OPOs) and amplifiers (OPAs) which are the important devices for the generation of optical squeezed states [1] and entangled states [2], [3]. These nonclassical states of light have been applied in the advanced experimental investigations of precision metrology [4] and quantum information [5]–[7]. There are two types of phase-matching in second-order nonlinear optical parametric processes, type-I (The polarization direction of the signal and idler light is identical.) and type-II (The polarization directions of the signal and the idler light are perpendicular each other) [8]. Since the two-mode squeezed states and the entangled states of light can be produced directly by a OPO or OPA with a type-II nonlinear crystal, the type-II phase-matching KTP ($KTiOPO_4$, Potassium Titanyl Phosphate) crystals have been efficiently utilized in the experimental systems of quantum optics and quantum information [2], [3], [9]. To achieve the generation of the squeezed and entangled states of light in OPOs or OPAs, through a frequency-down-conversion process, the OPOs (OPAs) have to be pumped by a single-frequency laser with a suitable wavelength which can satisfy the requirements for phase-matching in the nonlinear crystal. The laser at 532 nm can complete the optical parametric conversion with high efficiency in type-I phase-matching nonlinear crystals, such as PPLN (Periodically Poled Lithium Niobate), PPKTP (Periodically Poled KTP), LBO (Lithium Triborate), and so on, thus it has been extensively applied [10]–[14] and has had commercial products [14]. However the wavelength of 532 nm is not able to realize type-II non-critical phase-matching in KTP crystal at usual condition. Garmash *et al* reported the nonlinear optical process of 1080 nm-wavelength laser in an a-cut KTP crystal with type-II non-critical phase-matching [15]. Due to collinear transmission of the fundamental wave and the harmonic wave in the case, the effect of the beam walk-off was minimized, thus this work opened up a new opportunity for the application of the Nd:YAP (Yttrium Aluminum Perovskite) laser. In 1992, Ou et al demonstrated experimentally the Einstein-Podolsky-Rosen (EPR) paradox for continuous variables (CV) using a subthreshold OPO with a type-II KTP crystal pumped by a home-made frequency doubling Nd:YAP laser at 540 nm [2]. Subsequently, the group exploited the EPR beam to realize a two-channel quantum communication experiment and an improvement of 3.2 dB in signal-to-noise ratio was achieved over that possible with correlated classical sources [5]. Later, our group designed and built a single-frequency Nd:YAP laser operating at both wavelengths of 1080 nm and 540 nm, and the output powers of 1.1 W for the second-harmonic wave (540 nm) and 700 mW for the fundamental wave (1080 nm) were obtained [16], [17]. According to the requirements of developing quantum information network and quantum computation with optical CV, we have to prepare multipartite entangled states of optical beams firstly [18]. A set of four OPOs [19] or two nondegenerate OPAs (NOPAs) [9] pumped by a laser source has been successfully used for multipartite entangled state generation systems, which have produced four-partite entangled optical beams. Although optical beamsplitters can be utilized to directly generate multipartite entangled state in principle [20], unavoidable excess vacuum noises will significantly reduce the quantum entanglement unless each vacuum channel is filled by a squeezed vacuum [21]. Thus, more OPOs and OPAs pumped by a laser source have to be required for generating multipartite entangled optical beams with higher entanglement. From the experimental consideration there are two effort directions to build the multipartite entangled optical

Manuscript received December 23, 2010; revised March 13, 2011; accepted March 28, 2011. Date of current version June 17, 2011. This work was supported in part by the National Natural Science Foundation of China under Grant 61008001 and Grant 60736040, National Basic Research of China under Program 2010CB923101, and National High-Tech Research and Development of China under Program 2011AA030203.

The authors are with the State Key Laboratory of Quantum Optics and Quantum Optics Devices, Institute of Opto-Electronics, Shanxi University, Taiyuan 030006, China (e-mail: yhzheng@sxu.edu.cn).

Color versions of one or more of the figures in this paper are available online at http://ieeexplore.ieee.org.

Digital Object Identifier 10.1109/JQE.2011.2138681

sources: one is to reduce the oscillation threshold of OPOs and OPAs, and the other one is to raise the output power of the pumping laser. The threshold is limited by the losses of the nonlinear crystal and optical components. We paid a lot of efforts on raising the output power of the Nd:YAP laser. So far, the output powers up to 4.5 W at 540 nm and 1.5 W at 1080 nm have been achieved simultaneously with a laser source. The high power laser has been applied to pump more than four NOPAs in our lab and to produce the entangled state with more than eight optical beams, which can be applied in the experimental demonstration of complex CV quantum information network and quantum computation [22].

Usually, in a system of quantum optics and quantum information with OPO or OPA, the strong second-harmonic laser, such as at 532 nm or 540 nm, serves as the pump field to demonstrate the frequency-down-conversion in an optical cavity [2]–[4], [9]. On the other side the single-mode fundamental-wave laser, such as at 1064 nm or 1080 nm, is also needed, which provides the local oscillation light for homodyne-detectors and injected signal optical beams of OPOs or OPAs. For increasing the efficiency of the homodyne-detection and achieving the optimal mode-matching between the injected signal and OPOs or OPAs, the fundamental-wave laser has to pass through a mode-clearer firstly to filter the extra classical noises in the light field and to improve the quality of the transverse-mode of the light beam [4], [23]. The partial power of the fundamental wave will be lost in the mode-clearing process. Especially, in a complex quantum information network with multipartite entangled optical beams, more OPOs (OPAs) and more homodyne detectors are used [9], thus not only the high power second-harmonic wave is needed but also the intense fundamental wave is required. For obtaining high quality squeezed and entangled states of light the parametric conversion efficiency in OPOs and OPAs should be as high as possible [24]. Therefore, the pumping laser and the injected signal light should be a stable single-frequency TEM_{00} laser with a narrower linewidth to meet the requirements of phase-matching and mode-matching for the parametric process. For developing the optical quantum information network we design and build an intracavity frequency-doubling CW laser with a dual wavelength output at both 540 nm and 1080 nm. Comparing with the laser system using an external resonant cavity to implement frequency-doubling [25], the configuration of the intracavity frequency-doubling laser is relatively simple and compact.

In this paper, we will discuss the design characteristics of the high power Nd:YAP/LBO laser and present the experimental results. According to the optimal nonlinear coupling condition for the intracavity second-harmonic generation demonstrated by Smith et al [26] and Polloni et al [27], the parameters of the laser resonator are optimized. The thermo-optics coefficient of Nd:YAP crystal is much higher than that of Nd:YAG and Nd:YVO_4 crystal and thus there are possibly stronger thermal focusing and optical spherical aberration in Nd:YAP laser. In the design of high power Nd:YAP laser resonator it is a stringent requirement to mitigate the influence of the laser thermal effect. By choosing a lower doped YAP crystal (doping concentration 0.4%) and using a figure "8" shaped ring resonator consisting of two convex mirrors and two concave mirrors, which forms a larger spot size of the fundamental mode at the location of the laser crystal, the thermal effect in the crystal is significantly mitigated and the output power of the laser is increased, relative to our earlier work [16], [17]. In addition, for ensuring a stable polarization orientation of the fundamental wave and the unchanged unidirectional operation of optical beams in the high power laser, we inserted an additional wedge YVO_4 crystal into the resonator to be a polarized beam splitter, which improved greatly the stability of the laser. The main features of the presented laser: 1) The intense dual wavelength lasers of 4.5 W at 540 nm and 1.5 W at 1080 nm are achieved. 2) The ring resonator consisting of two convex mirrors and two concave mirrors and satisfying the optimal coupling condition is utilized in the intracavity frequency-doubling laser instead of usual configuration involving two plane mirrors and two concave mirrors [10], [11], [16]. 3) A wedge YVO_4 crystal in the resonator is used for suppressing the unexpected polarized modes to improve the stability of the laser. In the following, we will introduce the design of the laser resonator firstly in Section 2 and then present the experimental arrangement (Section 3) and results (Section 4). At last, a brief summary is given in Section 5.

II. Design of Laser Resonator

It has been theoretically demonstrated that there is an optical nonlinear coupling parameter (K_{opt}) in an intracavity frequency-doubling laser for reaching the maximal internal second-harmonic conversion efficiency [26]–[28], which is

$$K_{opt} = \frac{2L}{S_0} \tag{1}$$

where, L is the total linear loss of the fundamental wave during a circulating inside the laser cavity, S_0 is the saturation parameter of the laser medium ($S_0 = h\upsilon/\sigma\tau$, h-Planck constant, υ-the frequency of the light, σ-the stimulated emission cross section, τ-the lifetime of the laser energy level) [29]. Eq. (1) means that the magnitude of the nonlinearity required for optimum second-harmonic production only depends on L and S_0, and independent of the gain. Thus for a given loss and a laser medium, optimum coupling can be achieved for all values of gain and hence all power levels. For an intracavity frequency-doubling laser under perfectly phase-matching condition the nonlinear coupling parameter (K) can be expressed by [26]:

$$K = 4\left(\frac{\mu_0}{\varepsilon_0}\right)^{1/2} \frac{4\pi^2 d^2 l_c^2}{\lambda^2 n_1^2 n_2 c^2}\left(\frac{\omega}{\omega_0}\right)^2 \tag{2}$$

where μ_0 and ε_0 are the permeability and permittivity of free space, respectively, λ is the wavelength of the fundamental wave, d is the effective nonlinear coefficient of the nonlinear crystal, n_1 and n_2 are the indices of the fundamental and the harmonic wave, respectively, c is the speed of light, l_c is the length of the nonlinear crystal, ω and ω_0 are the radius of the fundamental wave spot in the laser medium and the radius of the laser waist in the nonlinear crystal, respectively. If Nd:YAP and LBO crystal are used for the laser medium and

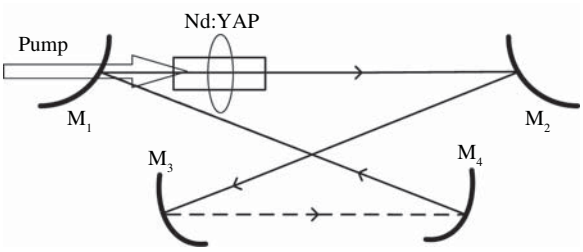

Fig. 1. Configuration of the laser resonator.

the nonlinear crystal respectively, we have approximatively $\lambda = 1.08\ \mu$m, $n_1 = n_2 = 1.56$, $d = 0.98$ *pm/V*. Substituting above values into Eq. (2) we obtain

$$K = 1.33 \times 10^{-8} l_c^2 \left(\frac{\omega}{\omega_0}\right)^2. \tag{3}$$

For Nd:YAP medium, $\sigma = 6.5 * 10^{-19}$ cm^2 and $\tau = 170\ \mu$s [29], thus S_0 =1.67*10^3 W/cm^2. To reach the optimal nonlinear coupling we should have $K = K_{opt}$ and thus from Eq. (1) and Eq. (3) we get

$$l_c^2 \left(\frac{\omega}{\omega_0}\right)^2 = 9 \times 10^3 L(cm^2). \tag{4}$$

If L = 3% and $l_c = 15$ mm (the case of our laser), when $l_c^2 \left(\frac{\omega}{\omega_0}\right)^2 = 270$ cm^2 and $\left(\frac{\omega}{\omega_0}\right)^2 = 120$ the optimal nonlinear coupling condition in the intracavity frequency-doubling laser will be satisfied. Besides considering the optimal coupling condition we also hope to make ω as large as possible with a view of the mode matching to reduce the thermal effect [30] in the laser medium with high power output [31]–[33].

Based on above theoretical analyses, we design a figure "8" shaped ring cavity (Fig. 1) consisting of two convex mirrors (M_1 and M_2) and two concave mirrors (M_3 and M_4). The curvature radius of both M_3 and M_4 is fixed at 100 mm and the length of the laser path outside M_3 and M_4 ($M_1 \rightarrow M_2 + M_2 \rightarrow M_3 + M_4 \rightarrow M_1$) is kept at 580 mm and is unchanged at all cases. The curvature radius of M_1 and M_2 is equal ($RM_1 = RM_2$) and are taken three different values in the numerical calculations and experiments. The Nd:YAP crystal is placed at the position close to the input mirror M_1 of the pump light, and LBO is put at an optimal position between M_3 and M_4 according to the calculated results. Using the distance (D) between M_3 and M_4 to be an adjustable parameter for the convenience of experiment, we calculate numerically ω and ω_0 and the distance (l) from the waist of the laser (ω_0) to M_4 as the functions of D for three different radius ($RM_1(M_2) = 1500$ mm, 3000 mm and ∞), which are shown in Fig. 2(a)–(c) respectively. In these calculations, the ABCD matrix and the condition of the laser stable mode operation, |A+D|<2, are applied [34]. The focal length of the thermal lens of the laser crystal is measured by means of the probe beam technique [35]. When the pump power and the spot radius of the pump light are 30 W and ~565 μm, the measured focal length of the thermal lens is about 150 mm. From Fig. 2 we can see, although the width of the stable region satisfying |A+D|<2 decreases when the

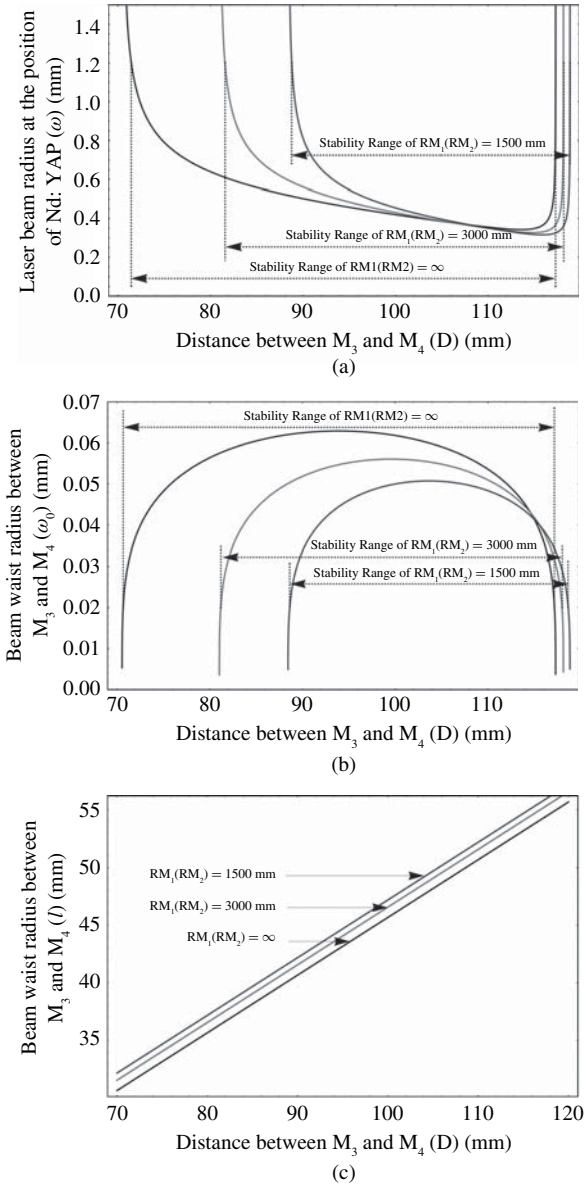

Fig. 2. Beam radius of fundamental wave (a) Nd:YAP. (b) LBO. (c) Beam waist position between M_3 and M_4 for three different radii of curvature of M1 and M2, RM1(M2) = 1500 mm, 3000 mm, and ∞.

curvature radius of M_1 and M_2 decreases, for a given distance between M_3 and M_4 inside the stable region the mode size (ω) at the position of Nd:YAP increases [Fig. 2(a)] and the radius (ω_0) of the beam waist between M_3 and M_4 decreases [Fig. 2(b)]. It is obvious that the larger ω and the smaller ω_0 can be obtained, if usual plane mirrors [$RM_1(M_2) = \infty$] [10], [11] are replaced by two convex mirrors. We prefer to choose $RM_1 = RM_2 = 1500$ mm, since if the curvature radius of M_1 and M_2 is further decreased the stable region of the laser operation is also narrowed, so the performance of the laser can not be further improved. From Fig. 2(a) and (b) we can see, when the distance of 96 mm between M_3 and M_4 is selected, $\omega = 517\ \mu$m and $\omega_0 = 0.47\ \mu$m. In this case, $\left(\frac{\omega}{\omega_0}\right)^2 = 120$ and $l_c^2 \left(\frac{\omega}{\omega_0}\right)^2 = 270$ cm^2 for $l_c = 15$ mm, thus the optimal

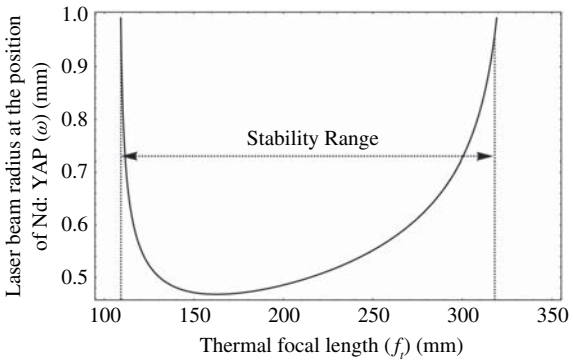

Fig. 3. Beam radius of fundamental wave in Nd:YAP as a function of thermal focal length of the Nd:YAP crystal.

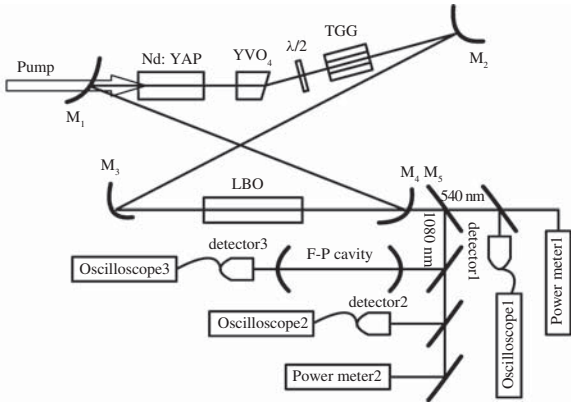

Fig. 4. Experimental schematic of the high-stability single-frequency Nd:YAP/LBO laser. $\lambda/2$: half wave plate, TGG: terbium gallium garnet.

coupling condition is reached. However, if the plane mirrors are used ($RM_1 = RM_2 = \infty$) the mode radius ω decreases from 485 μm to 430 μm and the radius ω_0 of the beam waist increases from 48 μm to 63 μm, where $\left(\frac{\omega}{\omega_0}\right)^2 = 46.6$, and $l_c^2\left(\frac{\omega}{\omega_0}\right)^2 = 105$ cm^2, which are far from the optimal coupling condition. On the curves of $RM_1(RM_2) = \infty$ in Fig. 2(a) and (b) we are not able to find a pair of ω and ω_0 values to satisfy the optimal coupling condition. Therefore, the design of the resonator with two convex cavity mirrors M_1 and M_2 ($RM_1 = RM_2 = 1500$ mm) not only can mitigate the thermal effects of the gain medium, but also can increase the frequency-doubling efficiency, Fig. 2(c) shows that for D = 96 mm and $RM_1 = RM_2 = 1500$ mm, the distance l from the waist spot ω_0 in the nonlinear crystal to M_4 should be 46 mm. To confirm the stability of the designed laser, we also calculate the function of ω_0 versus the thermal focal length f_t of the laser crystal (Fig. 3). Fig. 3 shows that if the thermal focal length f_t fluctuates in a range around 150 mm (about from 110 mm to 320 mm), the laser can still operate in the stable region ($|A + D| < 2$).

III. Experiment Arrangement

The experiment setup is shown in Fig. 4. The pump source of the laser is a commercially available fiber-coupled diode array (LIMO. Inc. HLU32-F400-DL803-EX826) with maximum output power of 32 W, which is the partially polarized light beams. The peak emission wavelength is temperature-tuned to the absorption peak of Nd:YAP crystal at 803 nm. The coupling fiber has a core diameter of 400 μm with a N.A of 0.22. The output of the fiber is focused by a focusing system, which consists of two lenses with focal lengths of 30 mm and 85 mm, respectively. The spot radius of the pump light imaged on the laser crystal is approximately 565 μm. In Ref. [32], [33] it has been pointed out that for reducing the diffraction loss of the pump light in high power lasers pumped by a fiber-coupled diode laser, the spot radius of the pump light can be larger than that of the laser. According to Ref. [32], when the ratio of the radius of the pump light and the radius of the laser does not exceed 1.2, the higher-order transverse modes can be suppressed. In the presented system the ratio of $\omega_{\text{pump}}/\omega = 567\mu\text{m}/485\,\mu\text{m} = 1.17 < 1.2$ and thus the single-mode operation can be achieved. Based on the discussion in Section II, a figure "8" shaped ring resonator is employed to construct the single frequency operation of the laser, where M_1 and M_2 are convex mirrors with 1500 mm radius of curvature as well as M_3 and M_4 are concave mirrors with 100 mm radius of curvature. In conventional intracavity frequency doubling lasers, all cavity mirrors are coated with high reflection at fundamental wave to achieve higher intracavity power of the fundamental wave. In our design, M_4 is coated with a 0.6% transmission at 1080 nm for obtaining dual wavelength outputs.

The gain medium of the laser is a Nd:YAP crystal of 3 mm-diameter and 15 mm-length with Nd concentration of 0.4%, which is placed behind the input mirror M_1 with a separation distance of 10 mm. Comparing with that used in Ref. [16], [17], the Nd:YAP crystal has lower doping concentration and longer length thus the thermal effect of the crystal is mitigated [13], [36]. The YAP crystal is cut along b-axis, the front end-face of which is coated with antireflective (AR) films for both wavelengths of 1080 nm and 803 nm and the second end-face is coated with AR films only for 1080 nm. Since Nd:YAP is a naturally birefringent crystal, the highest gain emission at 1080 nm is polarized parallel to the c-axis of the crystal cut along b axis, the laser will naturally be polarized in the superior direction usually. However, in the high power intracavity frequency-doubling laser the superior polarization mode of the fundamental waves is rapidly depleted during the frequency-up-conversion and thus its intensity in the resonator is drastically decreased. In this case some suppressed polarization modes before, such as a-axis polarization, will possibly start to oscillate, which will unavoidably affect the stability of the laser operation. In order to suppress the oscillation of other modes except the main polarization mode at the c-axis direction, Ref. [10] has used a Nd:YVO_4 crystal with a wedge shape end-facet of 1.5-degree to be the laser gain medium of a high power intracavity frequency-doubling laser. Based on the large birefringent property of the Nd:YVO_4 crystal, the transmission directions of the main polarization mode and other polarization modes are separated on the wedge shape end-facet of the laser crystal and thus the oscillation of those unexpected modes can be suppressed only by aligning

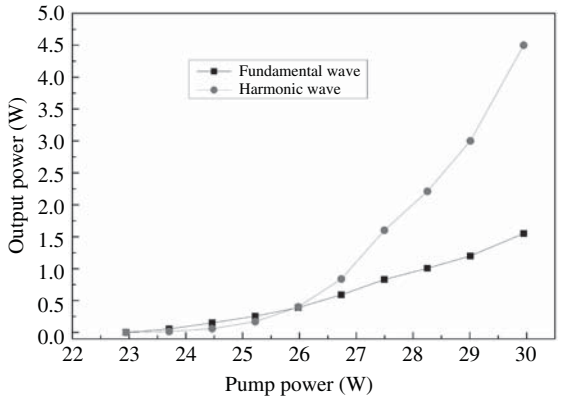

Fig. 5. Output power of the harmonic wave (circles) and the fundamental wave (square) vesus pump power.

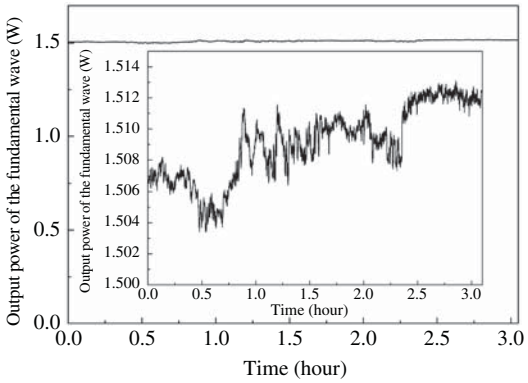

Fig. 6. Power stability of the fundamental wave in 3 h.

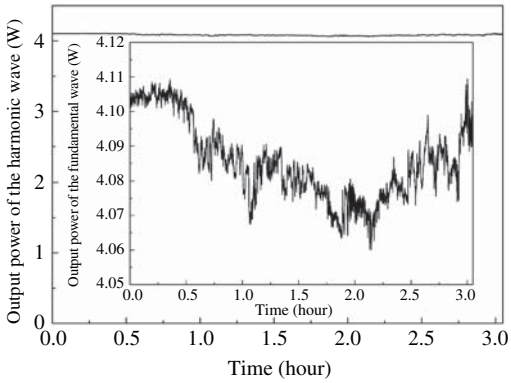

Fig. 7. Power stability of the harmonic wave in 3 h.

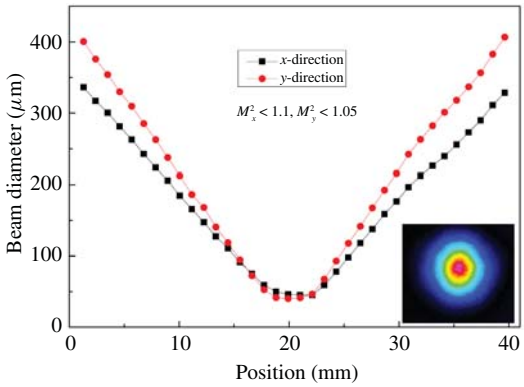

Fig. 8. Measured M^2 values and the spatial beam profile for 540-nm laser at the pump power of 30 W.

the desired main mode to resonate in the laser cavity. Ref. [10] shows, with respect to the similar Nd:YVO_4 laser but without using the wedge-shape crystal the stability of the laser with the wedge-shape crystal is improved significantly (the fluctuation of the output power is decreased from $\pm 1.2\%$ to $\pm 0.3\%$). However, differentiating from the Nd:YVO_4 crystal, the refractive indexes of the ordinary and the extraordinary light in the Nd:YAP crystal cut along b-axis are approximately the same [37], such that it is impossible to use the Nd:YAP crystal itself to be a polarizer by cutting a wedge on its an end-facet as that applied in Nd:YVO_4 lasers [10]. For suppressing the oscillation of other modes except main mode in the Nd:YAP laser, an additional YVO_4 crystal in a wedge shape is inserted inside the laser cavity to be a polarizer. The YVO_4 crystal is AR-coated at 1.08 μm with a measured residual reflection loss of 0.2%. Using the analysis model in Ref. [10], a wedge shape of 1.5-degree on an end-facet of the YVO_4 crystal is cut, which is enough to suppress the oscillation of other polarization modes and to enhance the superiority of the main polarization mode parallel to the c-axis in the mode competition under the present power level. After the YVO_4 optical wedge is inserted, the power stability of Nd:YAP laser is greatly improved relative to the earlier work [16], [17].

A LBO crystal of the dimensions of $3\times3\times15$ mm with type-I non-critical phase matching is used as the nonlinear crystal for the intracavity frequency-doubling and is placed to the position of the beam waist of the oscillating laser between M_3 and M_4. The LBO crystal is put in a copper oven, the temperature of which is controlled at the phase-matching temperature of 130° by use of a homemade temperature controller with the precision of 0.03°. The total length of the four-mirror ring cavity is approximately 678 mm. The mirror M_4 is mounted on a translator for changing the distance between M_3 and M_4 to adjust precisely the mode sizes in Nd:YAP and LBO crystals. The incident angles of the laser beams upon the folded cavity mirrors are set to be as small as possible for minimizing the astigmatism [38].

To maintain the unidirectional operation of the laser an optical diode consisting of a 10 mm-long terbium gallium garnet (TGG) rod and an AR-coated zeroth-order half-wave plate (HWP) at 1080 nm is applied. A magnetic field of 0.6 T is forced on the TGG rod to provide about 6-degree polarization rotation for the laser, which is enough to maintain a stable unidirectional lasing.

M_5 is a dichroic mirror coated with high reflection at 1080 nm and antireflection at 540 nm. A small part of reflected 1080 nm laser from M_5 is introduced into a Fabry-Perot (F-P) cavity with a free spectral range of 750 MHz to monitor the longitudinal mode of the laser and another small portion for detecting the short-term intensity fluctuation with the detector_2 and the oscilloscope_2 (or measuring the beam quality).

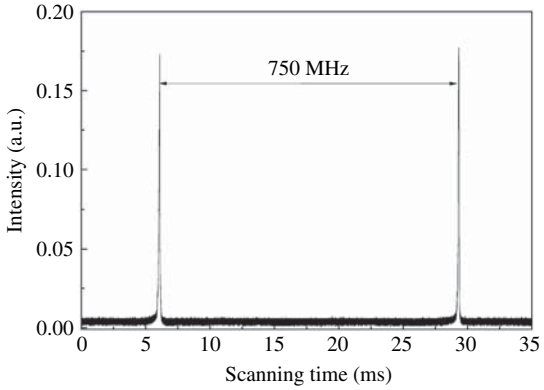

Fig. 9. Transmission intensity of the scanning confocal F-P interferometer. It indicates that the laser is in single-longitudinal-mode operation.

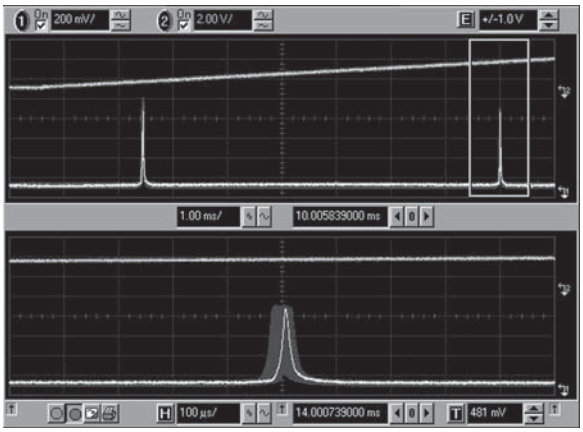

Fig. 10. Frequency shift of the fundamental wave in 15 minutes. The upper part shows the free spectral range (FSR) of the F-P cavity (the horizontal scale is 1 ms), the lower part shows the frequency shift of the laser (the horizontal scale is 100 μs). Using the FSR and the horizontal scale of the upper and lower parts, the frequency shift can be calculated.

The bandwidth of the detector is 1 GHz. The remainder with larger power is sent into the power meter$_2$ for the measurement of the output power of 1080 nm laser. A little green light at 540 nm leaked from M_5 is used for detecting the short-term intensity fluctuation by means of detector$_1$ and oscilloscope$_1$ as well as for measuring the beam quality.

IV. Experimental Results

According to the calculated results in Section II, the experiments are implemented mainly on the resonator with $RM_1 = RM_2 = 1500$ mm convex mirrors. For experimentally proving the superiority of the design some measurements on the resonators with $RM_1 = RM_2 = \infty$ and 3000 mm are also done, respectively. Under the pump power of 30 W both lasers with $RM_1 = RM_2 = \infty$ and 3000 mm can not operate with a single-mode and the multi-mode patterns of the output fundamental wave are always observed. Only when the pump power is smaller than 20 W the single-mode output can be obtained by the two lasers. The output powers at 540 nm (1080 nm) for $RM_1 = RM_2 = \infty$ and 3000 mm are 2.3 W (1.1 W) and 3.0 W (1.1 W) under the pump power of 30 W, respectively.

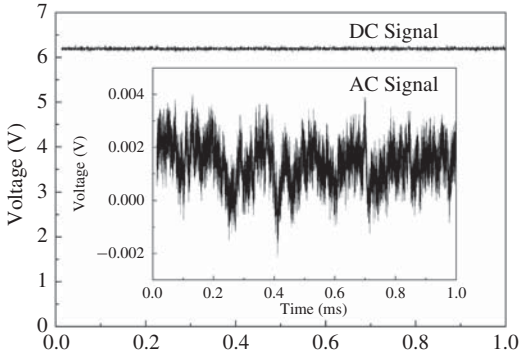

Fig. 11. Detected DC and AC signals for the fundamental wave.

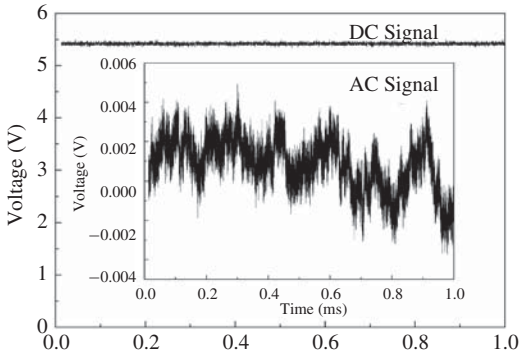

Fig. 12. Detected DC and AC signals for the harmonic wave.

When the convex mirrors of $RM_1 = RM_2 = 1500$ mm are used, we carefully adjust the distance D between M_3 and M_4 around the calculated optimal value of 96 mm in Section II and we find that the optimal conversion efficiency can not be obtained at D = 96 mm. However, the optimal operation is achieved at D = 98 mm. The reason of the small deviation appearing between the theoretical calculation and the experiment result is that the thermal focal length (150 mm) of the laser medium and the intracavity loss (3%) of the fundamental wave used in the calculations for ω and ω_0 values are not very precise. The deviations between the calculated and the real spot sizes results in the small deviation of D. We consider that the optimal coupling condition should be satisfied at D = 98 mm. Taking RM1 = RM2 = 1500 mm, D = 98 mm and l = 46 mm, the Nd:YAP/LBO laser can stably operate at single-mode with up to the pump power of 30 W. Fig. 5 shows the functions of the output powers of the fundamental wave and the second-harmonic wave versus the pump power. Under the pump power of 30 W, the output powers at 540 nm and 1080 nm are 4.1 W and 1.5 W, respectively, which are much larger than that obtained with RM1 = RM2 = ∞ and 3000 mm. The long term power stability of the laser is recorded by a power meter and data acquisition system, it is shown in Figs. 6 and 7. The power stabilities of the fundamental wave and the harmonic wave are $\pm$0.32% and $\pm$0.6% for 3 hours, respectively, without mode hopping. The beam quality of the laser is measured by a M^2 meter (DataRay. Inc).

The measured values of M_x^2 and M_y^2 at 540 nm (1080 nm) are 1.10 (1.11) and 1.05 (1.08), respectively. The measurement results for 540 nm are shown in Fig. 8 and the corresponding spatial beam profile is put in the inset of Fig. 8. The similar figure for 1080 nm is omitted. The transmission curve of the fundamental wave through a scanned F-P cavity (Fig. 9) demonstrates that the laser operates in a single-longitudinal mode. Using an electronic feedback frequency-locking system with a temperature-controlled F-P interferometer to be the frequency standard, the laser frequency is locked on. The frequency shift of the fundamental wave with the frequency-locking system on is better than ± 2.3 MHz in 15 minutes (Fig. 10). The inferred frequency shift of the second-harmonic wave should be better than ± 4.6 MHz in 15 min. The intensity noise of the infrared and the green laser measured with a fast silicon photo diode are 0.016% RMS (root mean square) (Fig. 11) and 0.03% RMS (Fig. 12), respectively. In Figs. 11 and 12, the upper smooth curve is the detected DC (direct current) signal, the lower black fluctuation curve is the detected AC (alternating current) signal, the intensity noise of light equals to the RMS of the AC signal divided by the average intensity of the DC signal. These signals are recorded by an oscillograph with different scales for DC and AC signals, respectively.

V. Conclusion

We design and construct a high power single-frequency Nd:YAP/LBO laser with dual wavelength outputs in which a figure "8" shaped ring cavity consisting of two convex mirrors and two concave mirrors is utilized. The cavity parameters of the laser resonator are optimized based on the numerically calculated results using the optimal nonlinear coupling condition for the intracavity second-harmonic generation, ABCD matrix and the laser stability condition. In the presented laser the optimal coupling condition is satisfied, thus the efficiency of the second-harmonic generation is enhanced. Besides, due to that the Nd:YAP crystal with lower doping concentration is chosen and the larger beam spot radius ω is obtained, the thermal effect in the laser crystal is mitigated. By inserting a wedge YVO_4 crystal in the resonator the unexpected polarizing modes are suppressed and thus the stability of the laser is greatly improved. According to our experiences, an all-solid-state continuous-wave single-frequency laser will reach a stable operating state after it stably operates for 2–3 hours and the stable state can last for a longer period unless the operation conditions are changed. We estimate that the designed laser can stably operate for 8 hours at least with the fluctuations of $\pm 0.5\%$ for 1080 nm wave and $\pm 1\%$ for 540 nm wave, respectively.

Due to the power limitation (32 W) of the LD pump source used in our experiments, the measurements on higher power have not been implemented. However, we consider that it is possible to increase the laser powers by further enhancing the pump power and lowering the intracavity loss. The presented configuration of the resonator can be a useful reference for the design of single-frequency solid-state-lasers with high power output. Of course, for lasers with higher powers the wedge angle on the YVO_4 crystal should be larger than 1.5° for completely suppressing those unexpected polarization modes according to Ref. [10].

References

[1] L. A. Wu, M. Xiao, and H. J. Kimble, "Squeezed states of light from an optical parametric oscillator," *J. Opt. Soc. Amer. B*, vol. 4, no. 10, pp. 1465–1475, 1987.

[2] Z. Y. Ou, S. F. Pereira, H. J. Kimble, and K. C. Peng, "Realization of the Einstein–Podolsky–Rosen paradox for continuous variables," *Phys. Rev. Lett.*, vol. 68, no. 25, pp. 3663–3666, 1992.

[3] Y. Zhang, H. Wang, X. Y. Li, J. T. Jing, C. D. Xie, and K. C. Peng, "Experimental generation of bright two-mode quadrature squeezed light from a narrow-band nondegenerate optical parametric amplifier," *Phys. Rev. A*, vol. 62, no. 2, pp. 023813-1–023813-4, Jul. 1999.

[4] H. Vahlbruch, M. Mehmet, S. Chelkowski, B. Hage, A. Franzen, N. Lastzka, S. Gobler, K. Danzmann, and R. Schnabel, "Observation of squeezed light with 10-dB quantum-noise reduction," *Phys. Rev. Lett.*, vol. 100, no. 3, pp. 033602-1–033602-4, Jan. 2008.

[5] S. F. Pereira, Z. Y. Ou, and H. J. Kimble, "Quantum communication with correlated nonclassical states," *Phys. Rev. A*, vol. 62, no. 4, pp. 042311-1–042311-8, Sep. 2000.

[6] S. L. Braunstein and P. V. Loock, "Quantum information with continuous variables," *Rev. Mod. Phys.*, vol. 77, no. 2, pp. 513–577, Jun. 2005.

[7] Y. M. Lian, C. D. Xie, and K. C. Peng, "Continuous variable multipartite entanglement and optical implementations of quantum communication networks," *New J. Phys.*, vol. 9, no. 9, p. 314, Sep. 2007.

[8] R. W. Boyd, *Nonlinear Optics*. New York: Academic, 2003, p. 97.

[9] X. L. Su, A. H. Tan, X. J. Jia, J. Zhang, C. D. Xie, and K. C. Peng, "Experimental preparation of quadripartite cluster and Greenberger–Horne–Zeilinger entangled states for continuous variables," *Phys. Rev. Lett.*, vol. 98, no. 7, pp. 070502-1–0705024, Feb. 2007.

[10] Y. H. Zheng, F. Q. Li, Y. J. Wang, K. S. Zhang, and K. C. Peng, "High-stability single-frequency green laser with a wedge Nd:YVO_4 as a polarizing beam splitter," *Opt. Commun.*, vol. 283, no. 2, pp. 309–312, Jan. 2010.

[11] K. I. Martin, W. A. Clarkson, and D. C. Hanna, "3 W of single-frequency output at 532 nm by intracavity frequency doubling of a diode-bar-pumped Nd:YAG ring laser," *Opt. Lett.*, vol. 21, no. 12, pp. 875–877, 1996.

[12] H.-T. Huang, G. Qiu, B.-T. Zhang, J.-L. He, J.-F. Yang, and J.-L. Xu, "Comparative study on the intracavity frequency-doubling 532 nm laser based on gray-tracking-resistant KTP and conventional KTP," *Appl. Opt.*, vol. 48, no. 32, pp. 6371–6375, 2009.

[13] L. McDonagh and R. Wallenstein, "Low-noise 62 W CW intracavity-doubled TEM_{00} Nd:YVO_4 green laser pumped at 888 nm," *Opt. Lett.*, vol. 32, no. 7, pp. 802–804, 2007.

[14] *Coherent Web Site* [Online]. Available: http://www.coherent.com/Lasers/index.cfmUTH

[15] V. M. Garmash, G. A. Ermakov, N. I. Pavlova, and A. V. Tarasov, "Efficient second harmonic generation in potassium titanate phosphate crystals with noncritical matching," *Sov. Tech. Phys. Lett.*, vol. 12, no. 4, pp. 505–506, 1986.

[16] X. Li, Q. Pan, J. Jing, C. Xie, and K. Peng, "LD pumped intracavity frequency-doubled and frequency-stabilized Nd:YAP/KTP laser with 1.1 W output at 540 nm," *Opt. Commun.*, vol. 201, nos. 1–3, pp. 165–171, Jan. 2002.

[17] Y. Yan, Y. Luo, Q. Pan, and K. C. Peng, "Watt level CW frequency-stabilized Nd:YAP/KTP laser with dual wavelength outputs," *Chin. J. Lasers*, vol. 31, no. 5, pp. 513–517, 2004.

[18] Y. Wang, H. Shen, X. L. Jin, X. L. Su, C. D. Xie, and K. C. Peng, "Experimental generation of 6 dB continuous variable entanglement from a nondegenerate optical parametric amplifier," *Opt. Exp.*, vol. 18, no. 6, pp. 6149–6155, 2010.

[19] M. Yukawa, R. Ukai, P. Loock, and A. Furusawa, "Experimental generation of four-mode continuous-variable cluster states," *Phys. Rev. A*, vol. 78, no. 1, pp. 012301-1–012301-6, 2008.

[20] P. Loock, C. Weedbrook, and M. Gu, "Building Gaussian cluster states by linear optics," *Phys. Rev. A*, vol. 76, no. 3, pp. 032321-1–032321-3, Sep. 2007.

[21] P. Loock and A. Furusawa, "Detecting genuine multipartite continuous-variable entanglement," *Phys. Rev. A*, vol. 67, no. 5, pp. 052315-1–052315-13, May 2003.

[22] M. Gu, C. Weedbrook, N. C. Menicucci, T. C. Ralph, and P. V. Loock, "Quantum computing with continuous-variable clusters," *Phys. Rev. A*, vol. 79, no. 6, pp. 062318-1–062318-16, Jun. 2009.

[23] M. Mehmet, S. Steinlechner, T. Eberle, H. Vahlbruch, A. Thüring, K. Danzmann, and R. Schnabel, "Observation of continuous-wave squeezed light at 1550 nm," *Opt. Lett.*, vol. 34, pp. 1060–1062, Feb. 2009.

[24] M. C. Scully and M. S. Zubairy, *Quantum Optics*. Cambridge, U.K.: Cambridge Univ. Press, 2003, p. 463.

[25] T. Meier, B. Willke, and K. Danzmann, "Continuous-wave single-frequency 532 nm laser source emitting 130 W into the fundamental transversal mode," *Opt. Lett.*, vol. 35, no. 22, pp. 3742–3744, 2010.

[26] R. Smith, "Theory of intracavity optical second-harmonic generation," *IEEE J. Quantum Electron.*, vol. 6, no. 4, pp. 215–223, Apr. 1970.

[27] R. Polloni and O. Svelto, "Optimum coupling for intracavity second harmonic generation," *IEEE J. Quantum Electron.*, vol. 4, no. 9, pp. 528–530, Sep. 1968.

[28] F. A. Camargo, T. Z. Willette, T. Badr, N. U. Wetter, and J. J. Zondy, "Tunable single-frequency Nd:$YVO_4BiB/_3O_6$ ring laser at 671 nm," *IEEE J. Quantum Electron.*, vol. 46, no. 5, pp. 804–809, May 2010.

[29] W. Koechner, *Solid-State Laser Engineering*. Herndon, VA: Springer-Verlag, 1999, p. 95.

[30] W. Xie, S.-C. Tam, Y.-L. Lam, H. Yang, J. Gu, G. Zhao, and W. Tan, "Influence of pump beam size on laser diode end-pumped solid state lasers," *Opt. Laser Technol.*, vol. 31, no. 8, pp. 555–558, Nov. 1999.

[31] Y. F. Chen, T. M. Huang, C. F. Kao, C. L. Wang, and S. C. Wang, "Optimization in scaling fiber-coupled laser-diode end-pumped lasers to higher power: Influence of thermal effect," *IEEE J. Quantum Electron.*, vol. 33, no. 8, pp. 1424–1429, Aug. 1997.

[32] X. Peng, L. Xu, and A. Asundi, "Power scaling of diode-pumped Nd:YVO_4 lasers," *IEEE J. Quantum Electron.*, vol. 38, no. 9, pp. 1291–1299, Sep. 2002.

[33] W. A. Clarkson, "Thermal effects and their mitigation in end-pumped solid-state lasers," *J. Phys. D: Appl. Phys.*, vol. 34, no. 16, pp. 2381–2395, 2001.

[34] H. Kogelnik and T. Li, "Laser beams and resonators," *Appl. Opt.*, vol. 5, no. 10, pp. 1550–1566, Oct. 1966.

[35] Y. F. Chen, Y. P. Lan, and S. C. Wang, "Influence of energy-transfer upconversion on the performance of high-power diode-end-pumped CW lasers," *IEEE J. Quantum Electron.*, vol. 36, no. 5, pp. 615–619, May 2000.

[36] E. Cheng, D. R. Dudley, W. L. Nighan, J. D. Kafka, D. E. Spence, and D. S. Bell, "Lasers with low doped gain medium," U.S. Patent 6 185 235, Feb. 2001.

[37] Z. Zeng, H. Shen, M. Huang, H. Xu, R. Zeng, Y. Zhen, G. Yu, and C. Huang, "Measurement of the refractive index and thermal refractive index coefficients of Nd:YAP crystal," *Appl. Opt.*, vol. 29, no. 9, pp. 1281–1286, 1990.

[38] Q. H. Xue, Q. Zheng, Y. K. Bu, F. Q. Jia, and L. S. Qian, "High-power efficient diode-pumped Nd:YVO_4/LiB_3O_5 457 nm blue laser with 4.6 W of output power," *Opt. Lett.*, vol. 31, no. 8, pp. 1070–1072, 2006.

Yajun Wang received the B.S. degree in physics from Shanxi University, Taiyuan, China, in 2008. He is currently pursuing the Ph.D. degree in all-solid-state single-frequency lasers at the Institute of Opto-Electronics, Shanxi University.

His current research interests include single-frequency lasers and nonlinear optics.

Yaohui Zheng was born in 1979. He received the M.S. degree in optical engineering and the Ph.D. degree in laser technology from Shanxi University, Taiyuan, China, in 2004 and 2009, respectively.

He is currently a Researcher at the Institute of Opto-Electronics, Shanxi University. His current research interests include high-power single-frequency lasers, quantum-optics devices, and nonlinear optics.

Changde Xie was born in 1939. She received the B.S. degree in physics from Sichuan University, Chengdu, China, in 1961.

She was a Visiting Scholar at the University of Texas, Austin, from 1982 to 1984, and from 1988 to 1989. Since 1990, she has been a Full Professor at the Institute of Opto-Electronics, Shanxi University, Taiyuan, China. Her current research interests include quantum computers, quantum information networks, and quantum optics devices.

Prof. Xie has been a fellow of the Optical Society of America since 2009, and is a member of the Chinese Physical Society.

Kunchi Peng was born in 1936. He received the B.S. degree in physics from Sichuan University, Chengdu, China, in 1961.

He was a Visiting Scholar at the University of Paris XI, Paris, France, from 1980 to 1982, the University of Texas, Austin, from 1982 to 1984, and the California Institute of Technology, Pasadena, from 1988 to 1989. Since 1990, he has been a Full Professor at the Institute of Opto-Electronics, Shanxi University, Taiyuan, China. His current research interests include all-solid-state laser technology, quantum information networks, and quantum optics devices.

Prof. Peng has been a fellow of the Optical Society of America since 2006, and is a member of the Chinese Physical Society.